Ministry of Higher Education
and Scientific Research

Journal of Kufa for Chemical Sciences

A refereed

Research Journal Chemical Sciences

Vol.2 No.9 Year 2022

ISSN 2077-2351

Removal o f Congo red by copoly (DMAEMA-AMPS) hydrogels for water treatment

Duha R. Abd-Alwahab, Salih H. Abbas and Athir M. Haddad*

Department of Chemistry, College of Science, University of Basrah, Basrah 61001, Iraq

الملخص

تم تحضير عشرة تراكيب هلامية كوبوليمرية من المونمرين 2- مثيل امينو ميثاكريليت و 2-اكريل اميدو- مثيل بروبان-1-حامض السلفونيك مع عامل التشابك المثيلين بس اكريل امايد باستخدم بلمرة الاكسدة – الاختزال. تم تشخيص الكوبوليمرات الهلامية بدراسة نسب الانتفاخ لها ودراسة الهيئة التركيبية لسطوح هذه الهلاميات باستخدام المجهر الالكتروني الماسح SEM ودراسة الهيئة المسامية والمساحة النسبية للسطح باستخدام تقنية BET. استخدمت هذ الكوبوليمرات الهلامية في ازالة صبغة الكونغو الاحمر من المحاليل المائية ووجد ان هنالك تركيبتين من التراكيب المحضرة (C20 و E20) اعطت افضل نتائج لازالة هذه الصبغة من المحاليل المائية أثبتت فعاليتها في إزالة هذه الصبغة عند دالة حامضية مساوية الى 7 اذ اظهر سلوك الامتزاز تطابقا مع نموذج فرندليش بالنسبة الى التركيبة C20 بينما التركيبة E20 تطابقت مع نموذج لانماير . وجد ايضا ان امتزاز صبغة الكونغو الاحمر على التركيبتين الهلاميتين يتبع حركية زائفة من الدرجة الثانية. نتائج طاقة التنشيط اظهرت ان الامتزاز للصبغة مع التركيبة البوليمرية C20 يكون ذو طبيعة امتزاز كيميائي في حين يكون امتزاز فيزيائي مع التركيبة E20 . أخيرًا أشارت دراسات استرجاع الصبغة (desorption) التي أجريت في 0.1 مولاري لكل من هيدروكسيد الصوديوم وحامض الهيدروكلوريك والماء المقطر و95% ايثانول إلى أن افضل مذيب لاسترجاع ولفظ الصبغة كان باستخدام هيدروكسيد الصوديوم.

Abstract

Ten copolymer gels were prepared from dimethylaminomethacrylate and 2-acrylamido-methylpropane-1-sulfonic acid with crosslinking agent methylene-bisacrylamide by redox polymerization. Hydrogels were characterized by studying their swelling ratios, the surface morphology by SEM, and studying the porosity and specific surface area by BET technique. The hydrogel copolymers were used to remove Congo red dye from aqueous solutions. It was found that there are two copolymers (C20 and E20) gave the best results for removing this dye from aqueous solutions at pH 7. The adsorption behavior was in agreement with Freundlich's model for C20, while E20 matched with Langmuir's model. It was also found that adsorption of Congo red dye on the two copolymeric hydrogels followed a order-second-pseudo kinetics. The results of the activation energy showed that the adsorption of the dye with the hydrogel C20 is chemisorption in nature, while it is physisorption with the hydrogel E20. Finally, desorption studies carried out in 0.1 M of

NaOH and hydrochloric acid, distilled water, and 95% ethanol indicated that the best eluent for dye recovery was NaOH.

Introduction:

Hydrogels are dimensional-three crosslinked polymeric networks with a porous framework that absorbs and retains a large amount of water. Swelling qualities can be found in one or more monomeric components. However, it does not dissolve in water. The inclusion of hydrophilic groups such as amino ($-NH_2$), hydroxyl (-OH) and carboxyl ($-COO^-$) functionalities in the polymeric network, contributes to the hydrogel capacity to retain water in its structure. Crosslinking between the polymer chains gives them resistance to disintegration[1]. Hydrogels are employed in a wide range of applications, including medication administration, contact lenses, solute separation, diapers, feminine hygiene products, agricultural and horticultural soil, water-blocking tapes, absorbent pads and others[2]. Apart from the various applications, it is clear that hydrogels have been widely employed as adsorbents for a long time, toxic metal ions and dyes are removed from the water medium. Dyes and pigments are frequently used to color items in a variety of industries, including textiles, plastics, paper, printing, leather, cosmetics, pharmaceuticals, and food[3]. The effluents produced by these industries are the primary source of water contamination[4]. The dyes in these effluents have mutagenic and carcinogenic consequences on aquatic organisms and humans[5]. Treatment of effluents containing synthetic dyes is problematic due to dyes’ stability in the presence of light and their resistance to degradation[6]. Various types of dyes, as well as their derivatives, are toxic to living beings. Congo red (CR) [1- naphthalene sulfonic acid, 3,4, 3’-(4,4’- biphenylene bis (azo)) bis (4- amino-) disodium salt] is an azo dye based on benzidine, it is poisonous and is used to color cotton, it exists as a brownish-red crystal that is air-stable. It serves as an indication by changing color from reddish-brown to blue in alkaline to acidic medium. Apart from its many uses, Congo red is harmful to humans and animals, as well as a threat to aquatic life. Even if only for a brief time when the dye comes into contact with the eyes, it creates a variety of irritations[7]. To date, scientists have shown a strong interest in adsorption treatment for wastewater as a possible candidate technique for dye wastewater purification[8,9]. Toxic dyes have been removed from wastewater using adsorbents such as graphene oxide[10], activated carbon[11], carbon nanotube[12], and nanocomposite hydrogels[13] without causing secondary contamination. Hydrogels are one of the most commonly used adsorbents to filter -dye contaminated effluents because of their high adsorption capacity, reusability, low cost, and ease of use[14–17]. In this study, several polymer hydrogels of the monomers DMAEMA (2 -(Dimethylamino) ethyl methacrylate) and AMPS (2-acrylamido-2-methylpropane sulfonic acid) and bis-acrylamide as a crosslinking agent were prepared with different ratios of monomers and the crosslinking agent. Swelling hydrogels and adsorption capacities were studied, and the best two hydrogels' formulations were selected as adsorbent surfaces and used to purity water contaminated with CR dye.

MATERIALS AND METHODS

Chemicals

Chemicals used in this study were obtained from different sources. 2-(methylamino) ethyl methacrylate, 2- acryl amido-2- methyl propane-1- sulfonic acid, N, N̍- methylenebisacryl amide and N, N, Ǹ, Ǹ- tetramethyl ethylene diamine (TEMED) were purchased from Sigma Aldrich, Germany. Sodium persulfate and Congo red dye were purchased from Fluka. Sodium hydroxide was supplied from Merck. Hydrochloric acid supplied by J.T. Baker.

Preparation of poly (DMAEMA- Co- AMPS) hydrogels:

Hydrogel copolymer A10 was prepared by dissolving (1 g) of 2dimethylaminoino) ethyl methacrylate and 2- acryl amido-2- methyl propane-1- sulfonic acid in (15 ml) distilled water with heating at 60 °C then (0.2 g) N, N̍- methylenebisacrylamide was added with stirring. Aqueous sodium persulfate (SPS) solution (1 gm SPS/10 ml water) and N, N, Ǹ, Ǹ- tetra methylethylenediamine (TEMED) were used as initiator and accelerator, respectively. Stirring continues for about 15 minutes until the polymerization process is completed and the hydrogel is formed. The resulting swollen hydrogels were washed several times with distilled water and dried in a vacuum oven at 40 ^{o}C. The copolymeric hydrogels A20 – E20 were prepared at the same procedure with different monomers ratios, as shown in Table 1. Scheme 1 shows the chemical equation of polymerization reaction.

Table 1. The composition of the prepared copolymer hydrogels

Hydrogel	DMAEMA (ml)	AMPS (gm)	N, Ǹ-methylenebisacryl amide (% $^{wt}/_{wt}$)
A10	1	1	10%
A20	1	1	20%
B10	2	1	10%
B20	2	1	20%
C10	3	1	10%
C20	3	1	20%
D10	1	2	10%
D20	1	2	20%
E10	1	3	10%
E20	1	3	20%

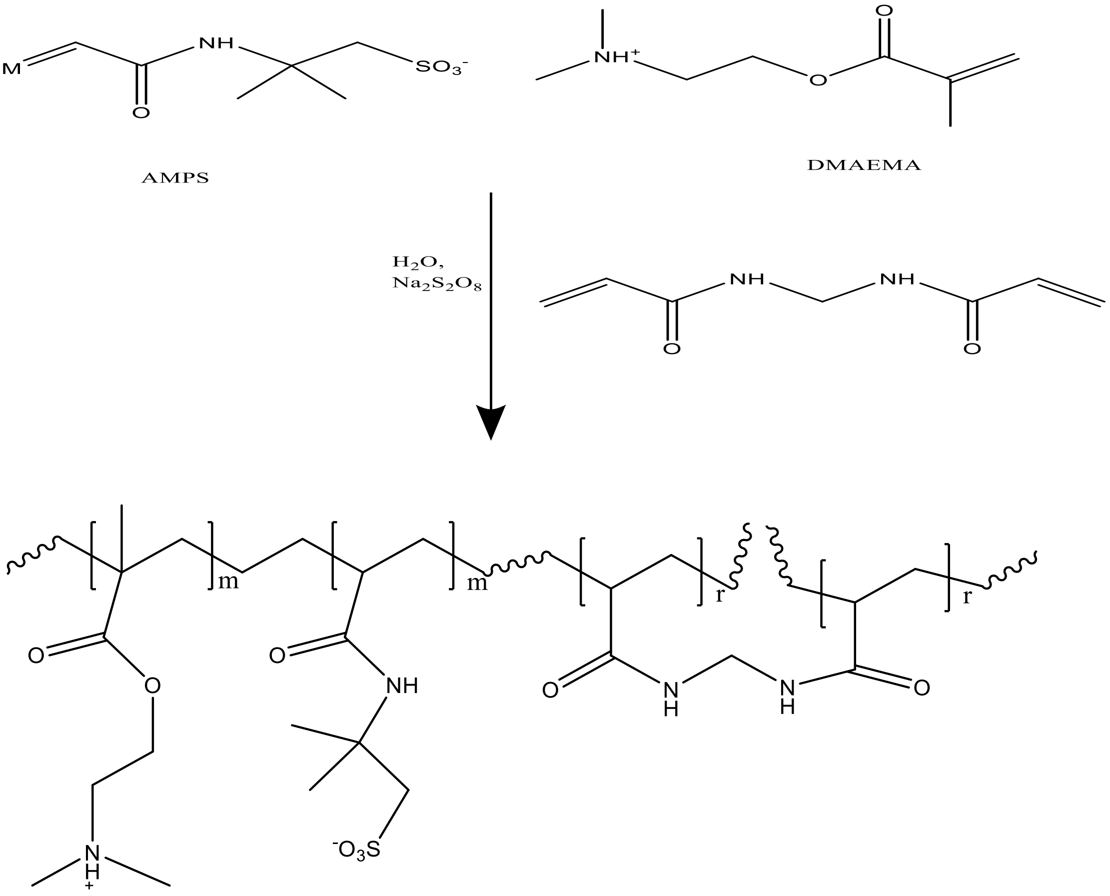

Scheme 1. Polymerization reaction for preparation of crosslinked copoly (DMAEMA- AMPS) hydrogels

Swelling studies

A pre-weighed dry hydrogel sample was immersed in 50 ml of deionized water at ambient temperature. After 24 hours, the samples were taken, wiped and weighed, and then the swelling ratio (Q) was calculated from the following equations[18,19]:

$$Q\% = \left(\frac{w_s - w_d}{w_d}\right) * 100\% \qquad [1]$$

$$Q = \frac{w_s - w_d}{w_d} \qquad [2]$$

Where W_s (g) and W_d (g) are the weight of swollen and dry hydrogel samples, respectively.

Preparation of aqueous dye solution

The stock dye solution was prepared by dissolving (1.0 g) of CR dye (Fig. 1) in DI water (1L) to give a concentration of 1.0 g. L^{-1}. The following dilutions of the dye stock solution in DI water were made to obtain the required concentrations in the work, which are (600 and 750) mg L^{-1}.

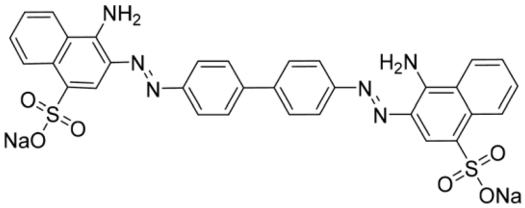

Figure 1. The molecular structure of Congo red dye[20]

Batch adsorption experiments

Batch adsorption experiments of CR were carried out to evaluate the adsorption parameters and factors influencing the adsorption. A total of (25.0 mg) of adsorbents C20 and E20 were placed in (100 ml) solutions (600 and 750 mg L^{-1} solution of CR). The adsorption experiments were conducted on a thermostat shaker at 25 ^{o}C, and the adsorption media was stirred magnetically at 225 rpm for a specific period of 60 min. After adsorption, the adsorbent was separated from the solution by simple filtration. The concentration of dye was determined by UV-Visible spectroscopy at the λ_{max} 494 nm. UV-Visible spectra were recorded by using T80^{+} spectrometer between 200 and 800 nm using a quartz cuvette with a path length of 1 cm. Adsorption experiments were carried out at optimum conditions applying an agitation time of 60 min at pH 7 . The concentration of CR dye on C20 and E20 adsorbent hydrogels was calculated using the following eqation[21,22].

$$q_e=\left(\frac{(c^{\circ}-C_e)}{w}\right)*v \qquad [3]$$

Where C^{o} and C_e (mg L^{-1}) are the initial and equilibrium concentration of dye in the solution, V (L) is the volume of solution, W (g) is the mass of hydrogel and q_e is the adsorption capacity (mg dye per g hydrogel).

In order to study the adsorption kinetics and to calculate the kinetic parameters enthalpy (ΔH°), entropy (ΔS°) and free energy (ΔG°), experiments were conducted at ambient temperature, 45 and 65 ^{o}C using (25 mg) of C20 and E20 in (100 ml) solutions of 600 and 750 mg L^{-1} of CR dye. By varying the pH of the dye solutions from 2 to 12, the maximum adsorption capacity was found at optimum pH. The pH of the dye solutions was adjusted using solutions of different concentrations (0.1, 0.2, 0.5, 1, 2 and 3 mol L^{-1}) of NaOH and HCl.

Desorption experiments

The desorption of dyes from the hydrogels was carried out by applying two adsorption/ desorption cycles of the same adsorbent. The maximum dye adsorption was accomplished by applying the optimum agitation time and pH for each dye-hydrogel combination. The desorption experiments were carried out by immersing dye-loaded adsorbent in DI water at pH 11, 0.1 M each of NaOH, HCl, and 95% ethanol and the mixture was stirred at 65 ^{o}C for 3 hours. The desorbed dye was separated by filtration and then the dye concentration in each solution was determined spectrophotometrically[23–25]. The removal efficiency of the CR dye was calculated using the following equation[26]:

$$S\% = \left(\frac{C_d\,V_d}{q_e\,W}\right) * 100\% \qquad [4]$$

Where S is the efficiency of dye desorption, C_d is the dye concentration in solution after desorption (mg L^{-1}) and V_d is the volume of the eluent (L).

Result and Discussion

The copolymeric hydrogels were prepared by Redox polymerization. One of the most significant parameters to consider when assessing the properties of hydrogels is their swelling capacity[24]. Hydrogels exhibit diversified swelling behaviors because of variation in hydrophilic functional groups, originating from different extents of added ingredients, temperatures, and methods of synthesis[27]. The swelling ratio of the prepared hydrogels was determined in distilled water at room temperature after being immersed in distilled water for 24 hours. Fig. 2 shows the swelling ratios of the hydrogels A10- E206. According to the results, the swelling ratio was increased with increasing in crosslinking density. The crosslinking agent reduces the polymer chain mobility, leading to decreased swelling ratios [27].

In the pH range of 2−12, AMPS remains dissociated. This is due to electrostatic repulsion between the ionized sulfonate groups which creates strong swelling driving forces at this pH range and hydrogel swells quickly. [28]. The swelling ratio of the hydrogels at a particular pH increases with increasing AMPS ratio within the copolymeric structure.

Figure 3 shows the XRD pattern of the copolymer E20 before and after adsorption with CR. Fig. 2 shows the same pattern, but different in the position and intensity of the peaks. This result indicates that the copolymeric hydrogel is still in the same phases but different in crystallinity properties. The intensity of the diffraction peak of hydrogel is higher before dye adsorption in comparison to their after dye adsorption and the lower intensity seen in adsorption state due to the disruption of the crystal structure of the copolymer backbone (DMAEMA-AMPS) as a result the dye adsorption, which appears in the change of the values of $2ɵ^{o}$ from 26.02 to 21.60.

SEM measurements were used to investigate the surface morphologies of the prepared hydrogels. Fig. (4A, 4B) show that the copolymeric hydrogels structures have rough surfaces and have many bumps on their surface in the dry state (xerogel). Fig. 4 (C-F) shows the swelling structures of the prepared hydrogels, which show large pore size as a result of its swelling, which allows the absorption of large amounts of water. It has cluster structures in the form of spherical or cubes and many of these structures are in the form of nanoparticles (Fig. 4G,4H).

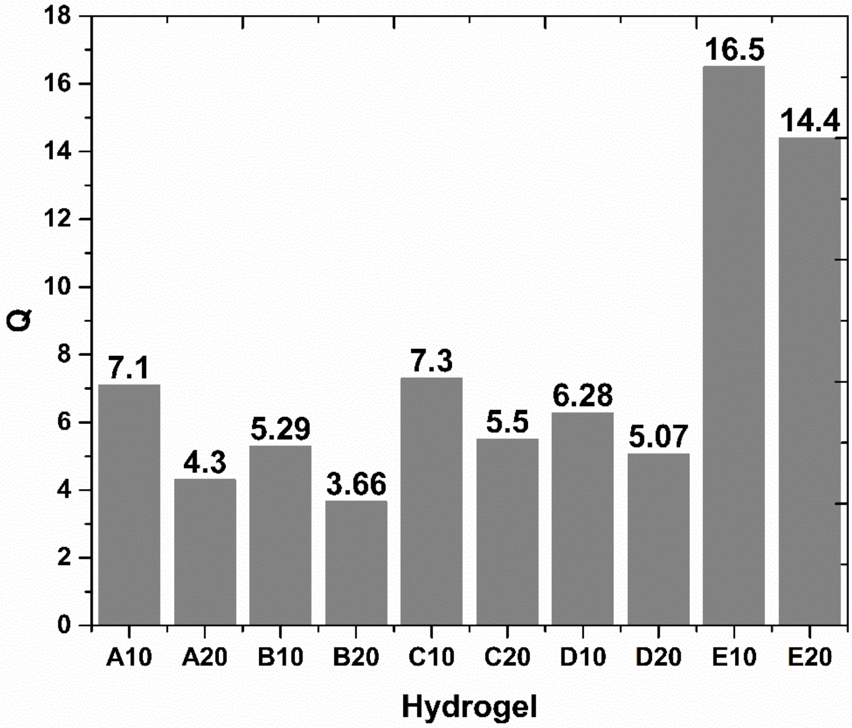

Figure 2. The swelling ratio of hydrogels A10-E20 in Distilled water.

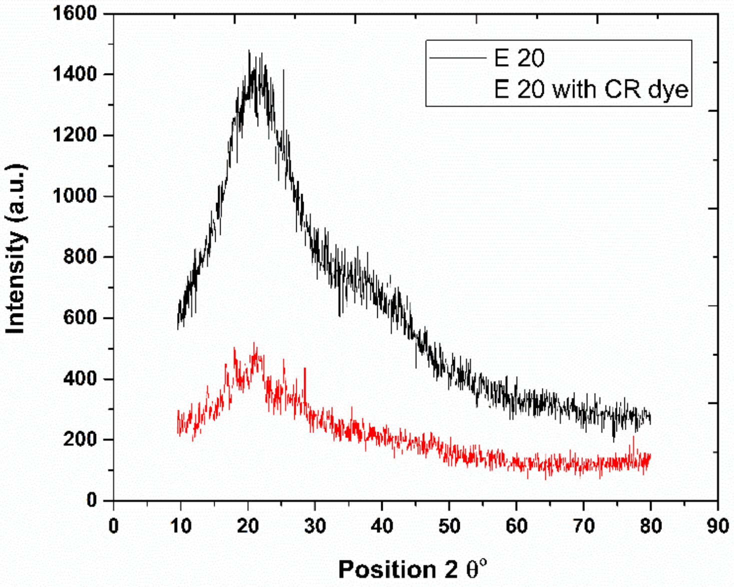

Figure 3. XRD diffraction pattern for copolymeric hydrogel before and after adsorption with CR dye

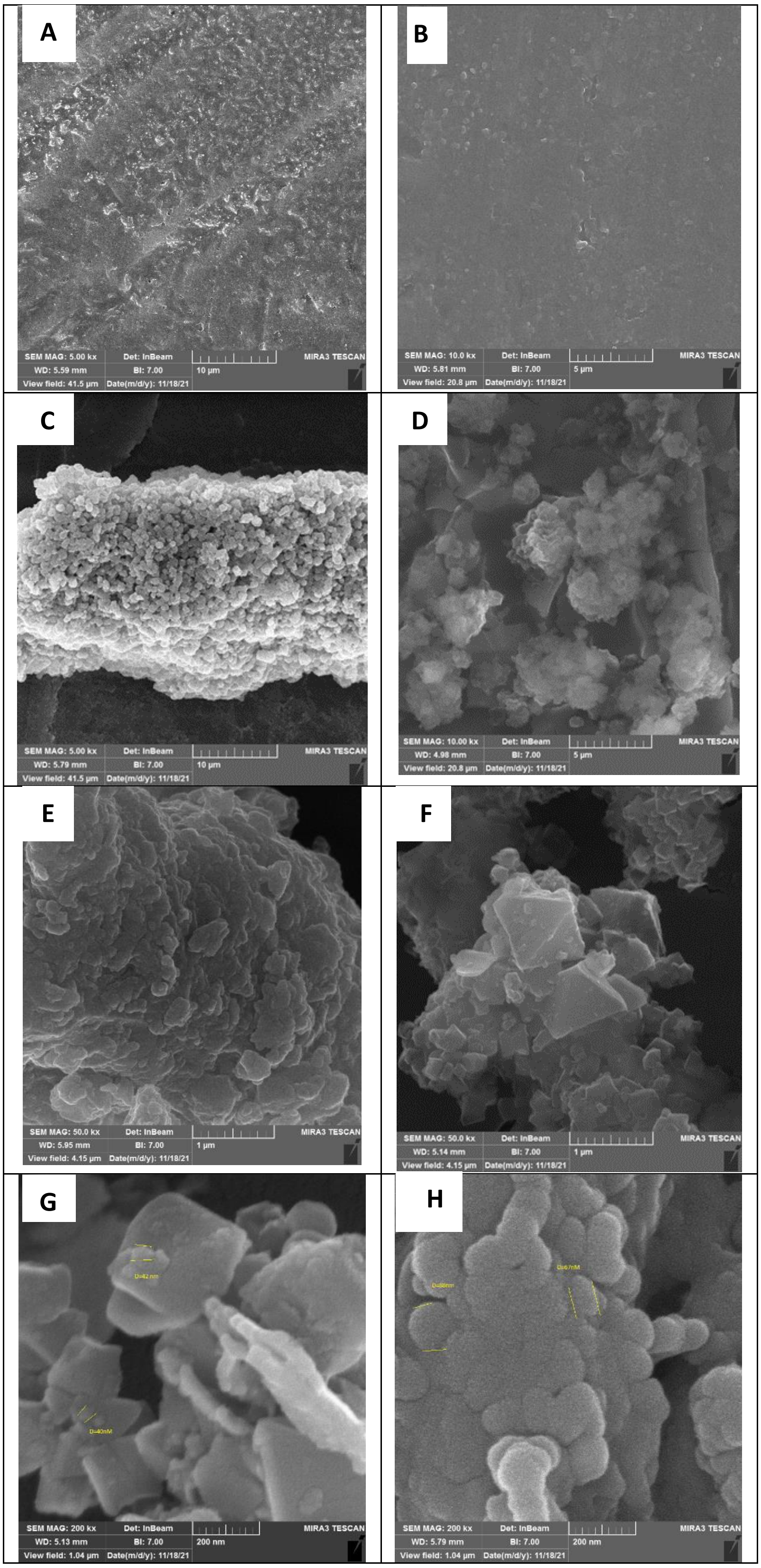

Figure 4. SEM of (A)The dry state E10 (Xerogel), (B) The dry state E20 (C) swelling state of the hydrogel B20 (D) swelling state of the hydrogel

A10 (E) swelling state of the hydrogel D20 (F) swelling state of the hydrogel C20 (G) Nanostructure of C20 (H) Nanostructure of B20

BET analysis was performed for hydrogels C20 and E20, Table 2 indicates the results from the BET analysis.

Table 2. The structure physical parameters of hydrogels C20 and E20

Hydrogel	Total specific surface area (m^2/g)	Mean pore diameter (nm)
C20	2.945	6.883
E20	1.7201	9.3236

The results indicate that the total specific surface area of the hydrogel C20 is greater than hydrogel E20 but it has a smaller pore size**,** this explains the higher swelling ratio of the hydrogel E20 and the mean pore diameter is more than 5 nm which indicate that the prepared copolymeric hydrogels are mesoporous materials. Hydrogel polymers have a large free volume within the swelling polymer chains, this increases its ability to adsorb metal, dyes and any active materials on its surface as well as within the inner network structure of the hydrogel. There are many are studies indicating that the hydrogel with high porosity and low surface area is better for metal and dyes adsorption compared to nanocomposites that have a higher surface area [29,30.]

Fig. 5 shows the adsorption/desorption of N_2 as a function of hydrogel particle size at 77 K. This sort of adsorption isotherm corresponds to type III of the BET classification[31], which describes the physical adsorption process of N_2. At higher relative pressures ($P/P_0 > 0.6$), the isotherms show remarkable hysteresis loops.

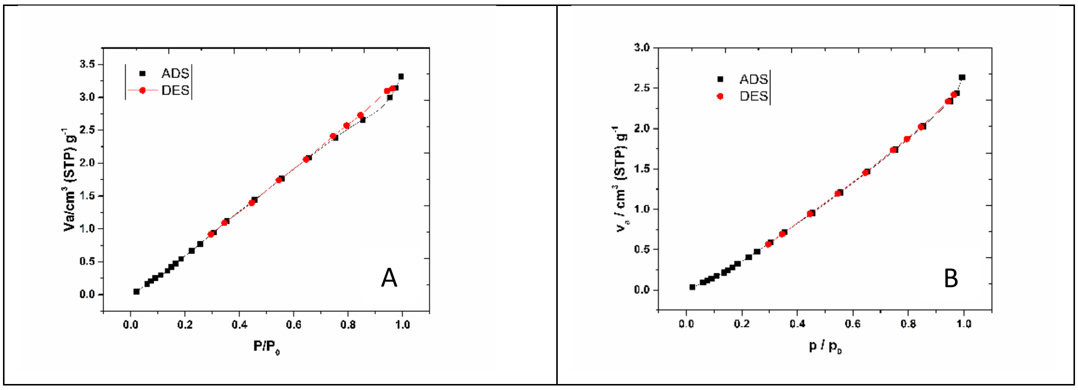

Figure 5. The N_2 adsorption-desorption isotherm of A) C20 and B) E20

The mesoporous nature of the hydrogels was confirmed by BJH pore size distribution curves (Fig. 6)[32].

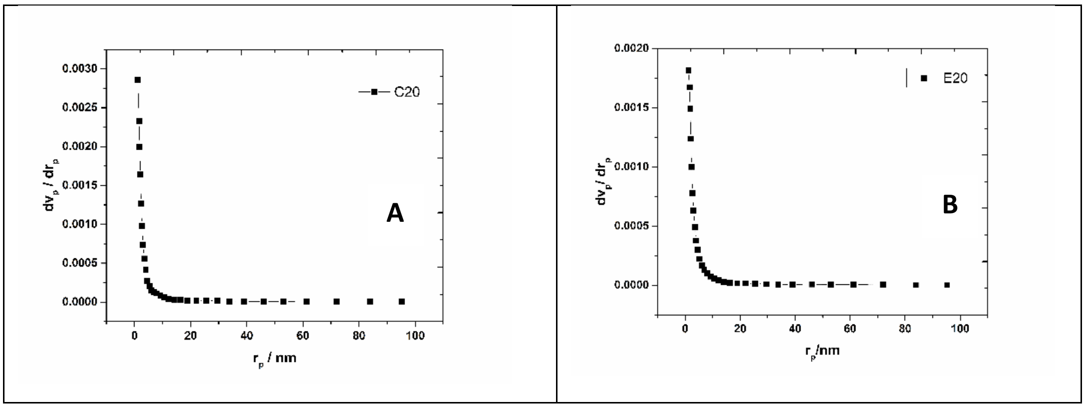

Figure 6. BJH pore size distribution of A) C20 and B) E20

TGA and DSC were used to investigate the thermal properties of the prepared copolymers; 10-20 mg of each copolymer sample was tested between 20 and 800 ^oC under N_2 gas at a constant heating rate of 10 ^oC min^{-1}. The initial decomposition temperature (T_i), the final decomposition temperature (T_f), the degree of decomposition temperature at 50% loss of sample weight ($T_{50\%}$) and char content at 800 ^oC were determined using TGA thermograms. The results are listed in Table 3 and Fig. 7.

The initial weight loss (between 100 ^oC -150 ^oC) was due to the loss of a little amount of water, which was attributed to the DMAEMA/AMPS copolymer networks' hydrophilicity[33]. Scission of the sulfonic acid residue is responsible for the first stage of decomposition and breaking the bonds between the carbon-nitrogen atoms, followed by the breaking of the carbonyl groups[34]. The second decomposition stage is due to copolymer chain decomposition[35].

There is just one T_g in Fig. 7A and 7B, which is obvious. The single peck of glass transition degree is an indication of the homogeneous distribution of monomers in the prepared copolymer, this indicates that there is no polymerization reaction from one of the components separately to produce a random copolymer, not a bulk copolymer[36]. Although the poly DMAEMA and poly AMPS have a low glass transition degree, the polymer prepared from them has a higher glass transition degree than them. This may be due to the interactions between the sulfonic groups with the amine groups, in addition to the crosslinking between the polymeric chains.

Table 3. The TGA results for prepared copolymers with their glass transition temperature from DSC

Copolymer	T_i (^oC)	T_f (^oC)	Weight loss ratio (%)	$T_{50\%}$ (^oC)	Rate of the decomposition (% wt.min^{-1})	Char content (%)	T_g* ^oC
C20				438		5	102
1st decomposition	291	370	30		0.283		
2nd decomposition	498	593	38		0.371		
E20				375		22	78
1st decomposition	297	363	32		0.712		
2nd decomposition	382	496	29		0.444		

Adsorption study

The adsorption performance of C10 and E20 towards CR dye was investigated by using batch system method experiments at optimum pH, contact time, temperature and initial concentration (Co) for CR dye. The important parameter influencing the hydrogels’ adsorption capability is pH. The effect of pH on dye adsorption capacity using these hydrogels was measured between pH 2.0 and 12.0. Fig. 8 illustrate the influence of the variation of pH on the adsorption capacities of C20 and E20, where they show the highest adsorption capacity in the strong acid medium at pH values of 2.0 and 3.0, but it was not actual adsorption, but a change in the composition of CR dye. This was confirmed by performing a spectroscopic scan of the dye at the above-mentioned pH values, which gave a new λ_{max} that differs from λ_{max} practically taken for the dye and mentioned in the literature. Fig. 8A shows the adsorption capacity of C20 increases with the decrease in pH of the anionic CR dye, the optimum pH value is 6.0, whereby the increase of hydrogen ions increases the electrostatic interactions between the negative charge of the anionic dye and the positively charged adsorption sites on the surface of the hydrogel. This is due to the protonation of the $-NH_2$ group which leads to an increase in the adsorption capacity.

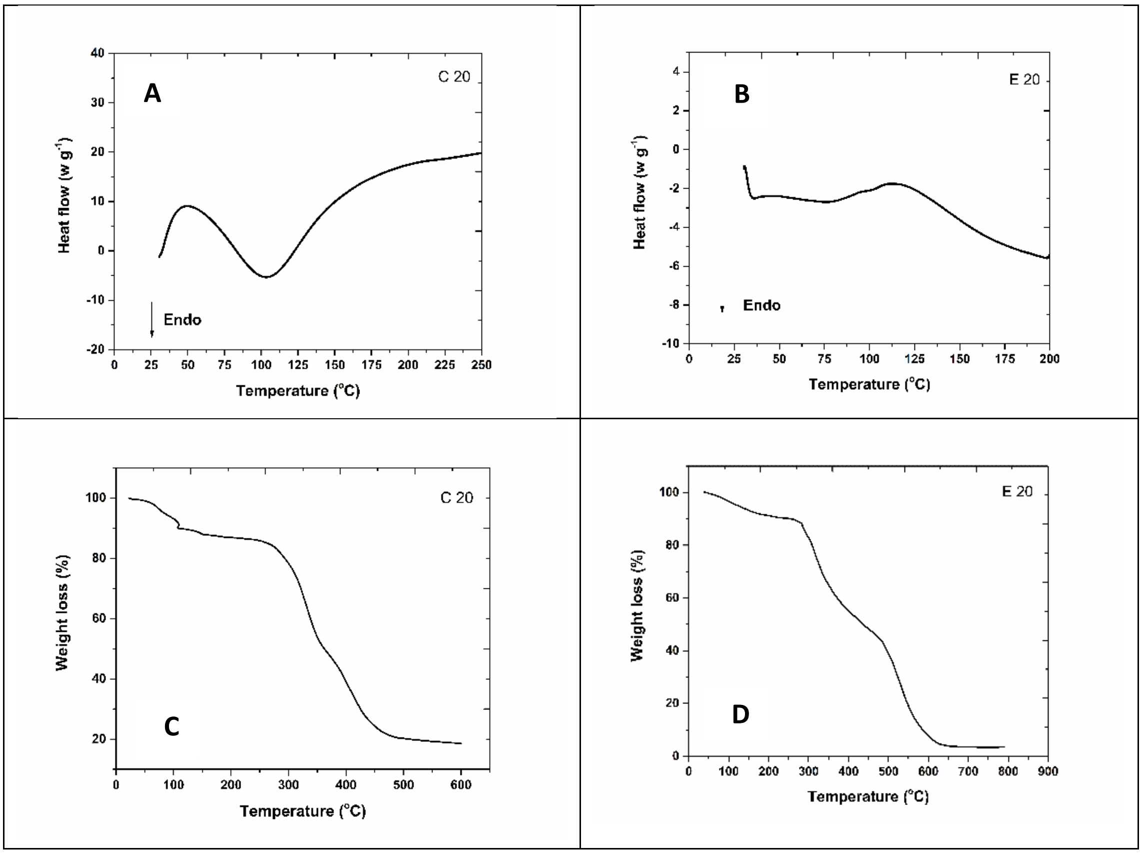

Figure 7. DSC thermogram of (A) C20; (B) E20; TGA thermogram of (C) C20; (D) E20

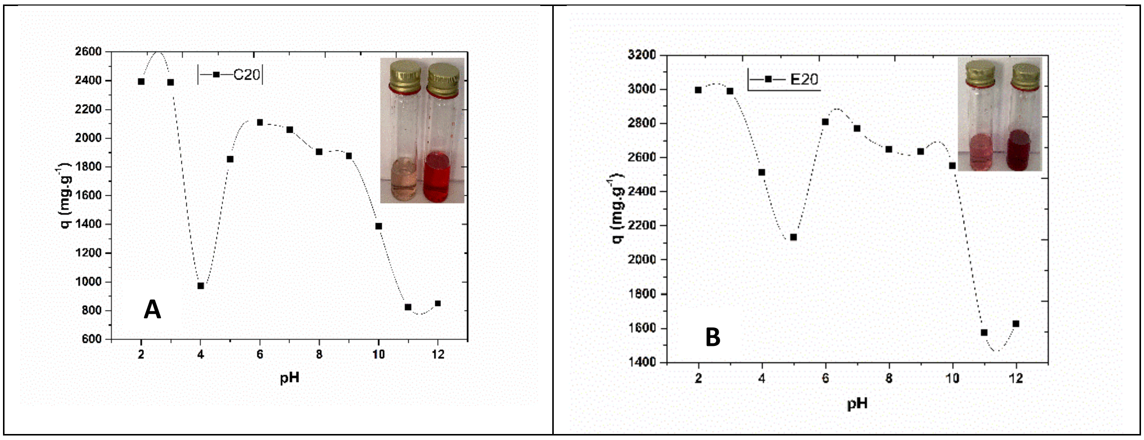

Figure 8. Effect of pH on the adsorption of CR dyes by hydrogels A) C20 and B) E20

Fig. 8B also shows the best adsorption capacity of CR dye in the neutral medium, where the optimum pH was 7. This is also a result of electrostatic interactions between the negative charge of the anionic dye and the positively charged adsorption sites represented by the ionized amino group present in the hydrogel.

The determination of optimum contact or agitation time [37] was carried out at diverse dye initial concentrations (100-750 mg L^{-1}) and the best initial concentrations of CR dye on C20 and E20 were found to be 600 and 750 mg L^{-1} respectively. Fig. 9 shows the plots for the effect of agitation time for the adsorption of CR dye at pH 7 onto adsorbent hydrogels at different temperatures. The adsorption of CR increased rapidly from 5 to 60 min for C20 and E20; 60 min is the equilibrium time that was determined when studying the adsorption of 180 min. The adsorption capacity decreases as the temperature increase (from 27 to 65 ^{o}C), therefore, the adsorption of CR is exothermic.

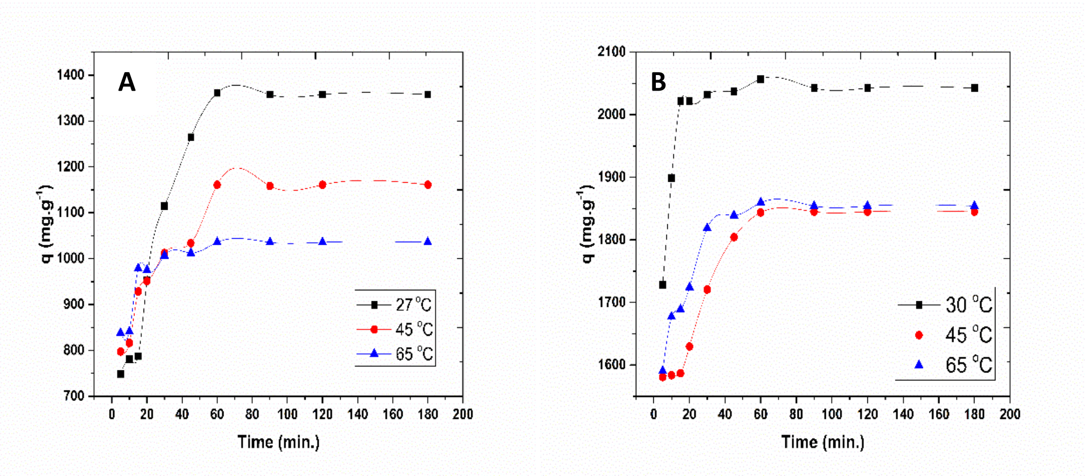

Figure 9. Effect of time on the adsorption of CR by hydrogels at pH 7.0 as a function of temperature A) C20 and B) E20

A comparison of the maximum adsorption capacity of **E20** with some reported adsorbents in the literature [7,38–40] for the removal of toxic CR dye is summarized in Table 4. The results in this table show that the values of adsorption capacity of **E20** are much better than some other reported adsorbents. This indicates that **E20** is an excellent absorbent and can be used for the removal of dyes from aqueous media.

To further comprehend the adsorption and explore the adsorption process mechanism, the adsorption equilibrium isotherms between adsorbents and adsorbate were studied at a fixed temperature of 30 ˚C. Adsorption data are generally described by adsorption models, such as Langmuir and Freundlich isotherms. The Langmuir is illustrated by the following equation[41]:

$$\frac{Ce}{qe} = \frac{1}{qmaxKL} + \frac{Ce}{qmax} \qquad [5]$$

Table 4. Comparison of maximum adsorption capacity of CR on E20 hydrogel adsorbent and other adsorbents.

Adsorbent	Adsorption capacity (mg/g)	Reference
Cetyl trimethyl ammonium bromide-chitosan	433.1	29
Zeolitic imidazolate framework-8	950	30
Chitosan hydro beads	93.4	28
Poly (N, N- dimethyl acrylamide –co-acryl amide) grafted hydroxyl ethyl cellulose hydrogel	102.4	7
E20 hydrogel	2057	This study

Where C_e (mg L^{-1}) is the dye concentration remaining in solution at equilibrium, q_e (mg g^{-1}) is the equilibrium concentration of dye adsorbed by the hydrogel, K_L (L mg^{-1}) is the Langmuir adsorption constant and q_{max} (mg g^{-1}) is the monolayer adsorption capacity of the hydrogel. The slope of the plot of C_e/q_e versus C_e is equal to $1/q_{max}$ and the Y-intercept is equal to $1/q_{max}$ K_L. The Langmuir equation is valid for monolayer adsorption of dye (adsorbate) onto the hydrogel surface
(adsorbent), and it assumes that there are restricted and homogeneous adsorption sites.64 The essential characteristics of a Langmuir isotherm can be expressed in terms of a dimensionless constant separation factor or equilibrium parameter R_L which is defined as [42]:

$$R_L = \frac{1}{1+KLC\circ} \qquad [6]$$

Where K_L is the Langmuir constant and C∘ is the initial concentration. The type of isotherm can be determined by RL values which indicate whether a sorption system is favorable ($0 < R_L < 1$) or unfavorable ($R_L > 1$). Fig.10 gives plots of the Langmuir adsorption isotherms of CR adsorbed onto hydrogels C20 and E20.

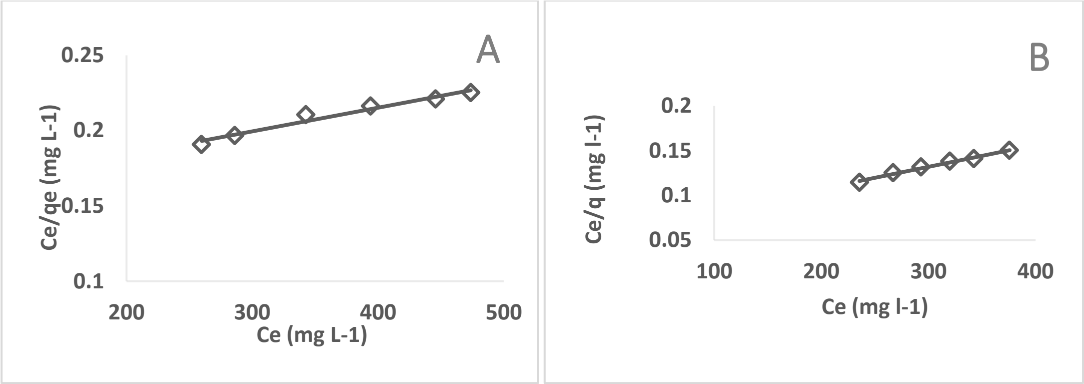

Figure 10. Langmuir isotherm model for the adsorption of CR dye at pH 7 A) concentration 600 mg L^{-1} by hydrogel C20 and B) concentration 750 mg L^{-1} by hydrogel E20.

The Freundlich isotherm is based on a heterogeneous exponentially decaying distribution, which fits well to the tailing portion of the heterogeneous distribution of the adsorbent. The general Freundlich isotherm can be defined as[43]:

$$lnq_e = lnK_f + \frac{1}{n} lnq\ C_e \qquad [7]$$

Where K_F (L mg^{-1}) is a constant for the adsorption or distribution coefficient and represents the amount of dye adsorbed onto the hydrogel at equilibrium concentration. Fig. 11 shows plots of the Freundlich adsorption isotherms of CR adsorbed onto the hydrogels.

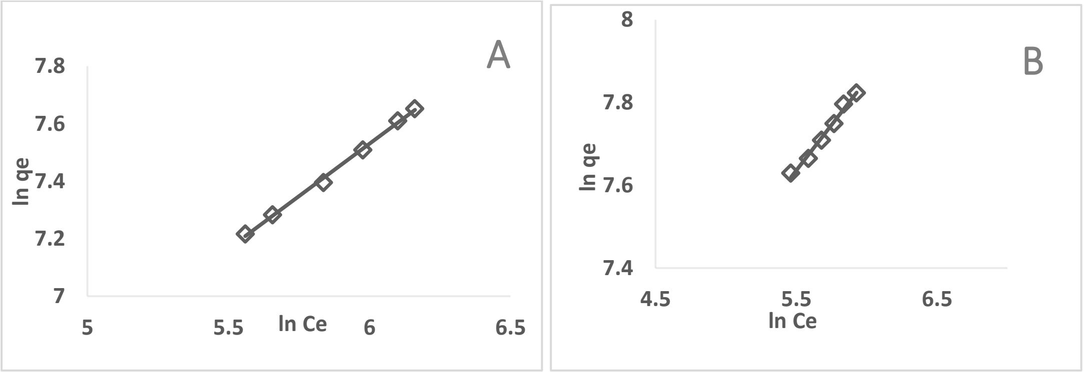

Figure 11. Freundlich isotherm model for CR dye at pH 7.0 A) concentration 600 mg L^{-1} by hydrogel C20 and B) concentration 750 mg L^{-1} by hydrogel E20.

Table 5 displays q_{max}, K_L, R_2 and the correlation coefficient results for the Langmuir isotherms. The calculated RL values of the CR dye onto **C20** and **E20** are found to be 0.559956 and 0.280576 respectively at an initial CR dye concentration of 600 and 750 mg L^{-1} adsorbed on **C20** and **E20** respectively. These results indicate that these hydrogels are favorable for adsorbing dyes from aqueous solutions under the optimized conditions applied in this study.

Table 5. Langmuir and Freundlich isotherm parameters for the adsorption of CR on C20 and E20 at 30 ˚C

	Langmuir isotherm			Freundlich isotherm		
Hydrogel	q_{max}(mg g^{-1})	K_L(L mg^{-1})	R^2	K_f(L mg^{-1})	1/n	R^2
C20	5000	0.00131	0.9647	23.5	0.7287	0.9974
E20	5000	0.003419	0.988	185.9	0.4383	0.9859

Table 5 displays also K_F, 1/n and the correlation coefficients which were determined from the linear plot of ln q_e versus ln Ce.

Three kinetic models were tested to interpret the mechanism of adsorption of CR dye onto the prepared hydrogels. The first model was pseudo-first-order; the mathematical expression of this model is given by[44]:

$$ln(q_e - q_t) = lnq_1 - K_1 t \qquad [8]$$

Where q_t and q_1 (mg g^{-1}) are the amounts of dye adsorbed at time t and equilibrium and K_1 (min^{-1}) is the pseudo-first-order rate adsorption constant.

A plot of $1/q_t$ versus 1/t gives the rate constants (K_1) and correlation coefficients.

Fig. 12 represents the pseudo-first-order equations for CR dye at different temperatures and the calculated K_1 and q_1 values are shown in Table 6.

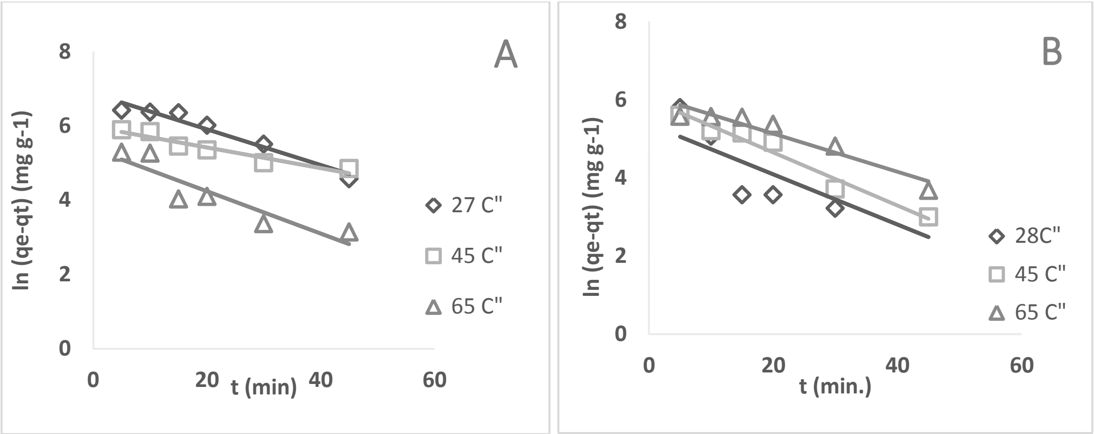

Figure 12. Pseudo-first-order kinetic plots for the adsorption of CR at pH 7; A) concentration 600 mg L⁻¹ on to C20 and B) concentration 750 mg L⁻¹ on to E20.

The second kinetic model was pseudo-second-order, which can be represented by the following equation[45,46]:

$$\frac{t}{q_t}=\frac{1}{K_2q^22}+\frac{1}{q2}t \qquad [9]$$

Where q_2 is the maximum adsorption capacity (mg g^{-1}) for pseudo-second-order adsorption and K_2 (g $mg^{-1}min^{-1}$) is the equilibrium rate constant for pseudo-second-order adsorption. Values of q_2 and K_2 were calculated from the slope and Y-intercept of the plot of t/q_t versusept t (Fig. 13). The kinetic data for the adsorption of CR dye onto the prepared hydrogels at various temperatures were calculated from the related plots and are summarized in Table 4.

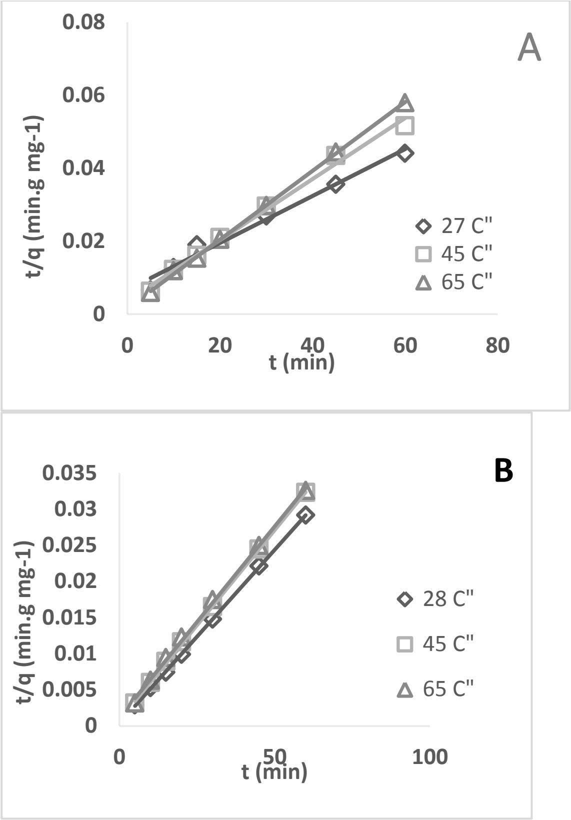

Figure 13. Variation of pseudo-second-order kinetic plots for the adsorption of CR at pH 7; A) concentration 600 mg L^{-1} onto C20 and B) concentration 750 mg L^{-1} onto E20.

Intra-particle diffusion was the final model investigated in this study; the intra-particle diffusion model equation is shown as[45–47]:

$$q_t = (K_p t^{1/2}) + C \qquad [10]$$

where C is the Y-intercept and K_p is the intra-particle diffusion rate constant ($mg^{-1}min^{-1/2}$) which were calculated from the slope of the plot of qt versus $t^{-1/2}$. Fig. 14 displays the intra-particle diffusion model for CR dye at different temperatures and Table 4 shows the calculated K_p and C values.

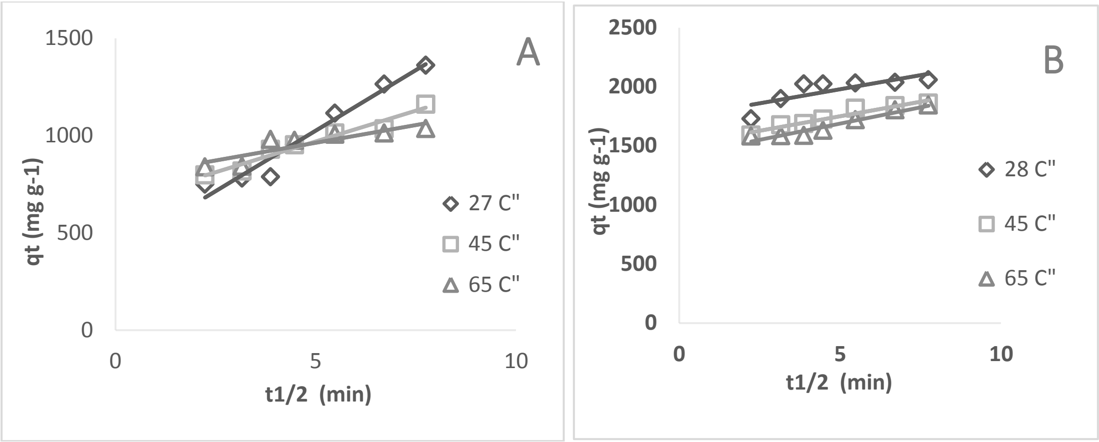

Figure 14. Intra-particle diffusion kinetic plots for the adsorption of CR at pH 7.0 A) concentration 600 mg L⁻¹ on to C20 and B) concentration 750 mg L⁻¹ on to E20.

Table 6. kinetic parameters for the adsorption of CR dye onto C20 and E20 at constant pH and different temperatures.

		Pseudo-first-order			Pseudo-second-order			Intra-particle diffusion		
Hydrogel	T	K_1	q_1	R_1^2	K_2	q_2	R_2^2	k_p	c	Rp²
C20	27	0.0483	968.35	0.9531	2.45×10^{-9}	1666	0.9779	124.39	403	0.9567
	45	0.0279	395.24	0.9173	2.37×10^{-9}	1250	0.992	63.174	653	0.9495
	65	0.0479	217.76	0.803	1.38×10^{-9}	1111	0.9994	36.43	780	0.7644
E20	28	0.064	214.5	0.6906	1×10^{-10}	2000	0.9999	47.8	1740	0.6185
	45	0.0678	405.16	0.9651	2×10^{-10}	2000	0.9997	49.2	1505	0.9397
	65	0.0488	448.7	0.9086	3×10^{-10}	2000	0.9983	54.8	0.933	0.933

T(˚C), q (mg g^{-1}), k_1, k_2: (g mg^{-1} min^{-1}), k_p: (mg g^{-1} $min^{-1/2}$).

As is evident from the correlation coefficients in Table 6, the CR dye adsorption systems follow the pseudo-second-order model and K_2 values for **E20** increase with an increase in temperature, while K_2 values for **C20** decrease with increase in temperature. However, the K_2 values were not always directly proportional to temperature. Thermodynamic parameters can be determined from the thermodynamic equilibrium constant KL (or the thermodynamic distribution coefficient) and are expressed in the following equation[48]:

$$KL = C_a/C_e \qquad [11]$$

where C_a and C_e are the equilibrium concentrations of CR dye onto **C20** and **E20**, as an adsorbent (mg g^{-1}) and in the solution (mg L^{-1}). The standard enthalpy change ΔH° (kJ mol^{-1}) and the standard entropy change ΔS° (J mol^{-1} K^{-1}) were calculated using the following equation[38]:

$$\ln k = \frac{\Delta S^\circ}{R} - \frac{\Delta H^\circ}{RT} \qquad [12]$$

Where R is the universal gas constant (8.314 J mol^{-1} K^{-1}) and T is the absolute temperature. ΔH° was obtained from the slope of the plot of ln KL versus 1/T (K^{-1}) and ΔS° was obtained from the Y-intercept for the adsorption of CR dye. The standard Gibbs free energy ΔG° (kJ mol^{-1}) was calculated at different temperatures, as listed in Table 7, from the following equation[45,48]:

$$\Delta G^\circ = \Delta H - T\Delta S^\circ \qquad [13]$$

Table 7. Thermodynamic parameters for the adsorption of CR dye onto C20 and E20 at different temperatures.

Hydrogel	T (K)	ΔH° (kJ mol^{-1})	ΔS° (J mol^{-1} K^{-1})	ΔG° (kJ mol^{-1})
C20	300.15	-25.2887	-89.4919	1.5723
	318.15			3.1832
	338.15			4.973
E20	301.15	-12.393	-45.0843	1.1843
	318.15			1.195
	338.15			2.852

The calculated thermodynamic parameters listed in Table 7, show negative values of enthalpy changes (ΔH°) for CR dye, indicating that the adsorption processes were exothermic. The negative values of the adsorption entropy (ΔS°) for the adsorption CR onto the prepared hydrogels indicate a decrease in the randomness at the adsorbent/solution interface and affinity of the prepared hydrogels towards this dye.

The free energy change (ΔG°) values for CR dye onto **E20** adsorbent are negative and increase with increasing temperature, denoting that the adsorption processes proceed spontaneously and reversibly, while CR onto **C20** hydrogel, (ΔG°) values are positive and increase with increasing temperature, this means that the adsorption non-spontaneous processes and irreversibly.

Desorption Studies

To make the adsorption process more economical, it was expedient to regenerate the used adsorbent and dyes, which could be recycled further [49]. Understanding the adsorption mechanism of adsorbate onto an adsorbent requires desorption investigations. Desorption of CR dye from C20 and E20 hydrogels by different eluents (distilled water, NaOH, HCl, is presented in Fig. 15.

The highest desorption percentage of the anionic dye from the surface of the hydrogels was using NaOH solution, where they were (24.5%) from **C20** surface, (67.5% and 20%) for the first and second cycles, respectively from **E20** hydrogel. Thus, the reduction in positively charged adsorption sites in alkaline solution led to the electrostatic repulsion of the anionic dye from the surfaces of **C20** and **E20.** Anionic dyes were chemisorbed onto the surface of cationic surfactant-modified adsorbents, as evidenced by the low percentage of desorption[50,51]. If the dye is desorbed in an alkali solution, the dye may be attached to the adsorbent by ion exchange or electrostatic attraction[52]. If an organic solvent, such as alcohol, desorbs the dye, chemisorption may be the cause of the dye's adsorption on the adsorbent.

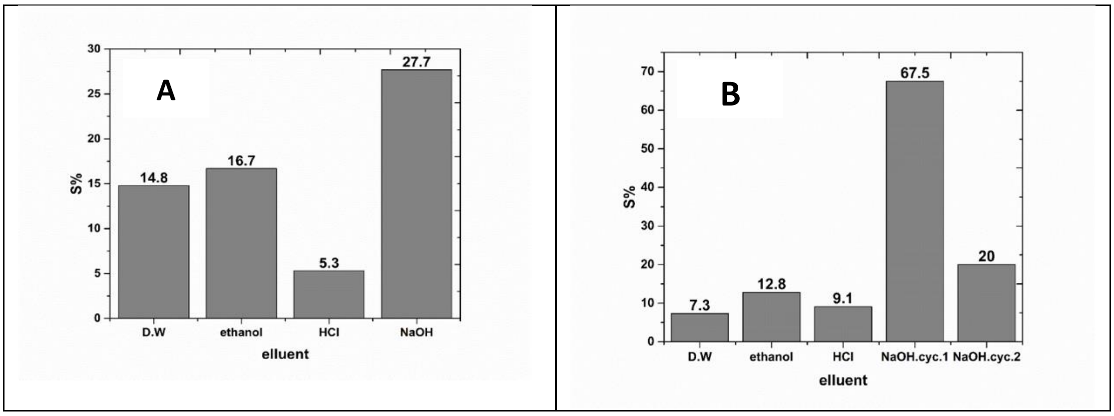

Figure 15. Desorption of CR dye from (8C) C20 and (8E) E20 hydrogels by different eluents.

Conclusion

The results showed that the prepared copolymeric hydrogels surfaces are effective for the adsorption of anionic dyes. The results showed that the pH affects the adsorption process, as the adsorption rate of anionic dyes (CR) increases in the acidic medium at the pH 6 or neutral function. The adsorption isotherm diagrams were studied using Langmuir and Freundlich models and it was found that the Langmuir model is more suitable for the experimental data for adsorption of CR dye on the surface of the prepared hydrogel E20. Either the adsorption process of CR dye on the surface of the prepared hydrogel C20 was followed to the Freundlich model.

References

1. Haddad, A. M., Al Asadi, I. J. & Falih, I. a Q. [2017]: Preparation of Nano Triblock Co-polymer for Desferoxiamine Delivery and Cross-Linked Copolymer for Iron Overload Disease. *Polym. Sci.* **03**.
2. Haddad, A. M., Sweah, Z. J. & Lami, H. S. Al.[2017]: Preparation and Release Study of Biodegradable L-lactide IPN's Insulin Delivery. *Polym. Sci.* **03**.
3. Kaykhaii, M., Sasani, M. & Marghzari, S [2018]: Removal of Dyes from the Environment by Adsorption Process. *Chem. Mater. Eng.* **6**, 31–35.
4. Arslan, C., Hasnain, M. & Tariq, W. [2021]:Environmental Contaminants Reviews (ECR) EFFECTIVE REMOVAL OF TEXTILE DYES USING PRE-TREATED NATURAL ADSORBENTS. **4**, 1–5 .
5. Crini, G. [2006]:Non-conventional low-cost adsorbents for dye removal: A review. *Bioresour. Technol.* **97**, 1061–1085.
6. Banerjee, S. & Chattopadhyaya, M. C. [2017]:Adsorption characteristics for the removal of a toxic dye, tartrazine from aqueous solutions by a low-cost agricultural by-product. *Arab. J. Chem.* **10**, S1629–S1638.
7. Jana, S., Pradhan, S. S. & Tripathy, T. [2018]:Poly(N,N-dimethylacrylamide-co-acrylamide) Grafted Hydroxyethyl Cellulose Hydrogel: A Useful Congo Red Dye Remover. *J. Polym. Environ.* **26**, 2730–2747.
8. Ozay, O., Ekici, S., Baran, Y., Aktas, N. & Sahiner, N. [2009]:Removal of toxic metal ions with magnetic hydrogels. *Water Res.* **43**, 4403–4411.
9. Shen, C., Shen, Y., Wen, Y., Wang, H. & Liu, W. [2011]:Fast and highly efficient removal of dyes under alkaline conditions using magnetic chitosan-Fe(III) hydrogel. *Water Res.* **45**, 5200–5210.
10. Soleimani, K., Tehrani, A. D. D. & Adeli, M. [2018]:Bioconjugated graphene oxide hydrogel as an effective adsorbent for cationic dyes removal. *Ecotoxicol. Environ. Saf.* **147**, 34–42.
11. Caicedo, O. D., Vargas, D. P., Giraldo, L. & Carlos Moreno-Piraján, J. [2021]:Study of Mercury [Hg(II)] Adsorption from Aqueous Solution on Functionalized Activated Carbon. doi:10.1021/acsomega.0c06084.

12. Ai, L. & Jiang, J. [2012]:Removal of methylene blue from aqueous solution with self-assembled cylindrical graphene–carbon nanotube hybrid. *Chem. Eng. J.* **192**, 156–163.
13. Hosseinzadeh, H. & Ramin, S. [2018]: Fabrication of starch-graft-poly(acrylamide)/graphene oxide/hydroxyapatite nanocomposite hydrogel adsorbent for removal of malachite green dye from aqueous solution. *Int. J. Biol. Macromol.* **106**, 101–115.
14. Li, S., Zhang, H., Feng, J., Xu, R. & Liu, X.[2011]:Facile preparation of poly(acrylic acid–acrylamide) hydrogels by frontal polymerization and their use in removal of cationic dyes from aqueous solution. *Desalination* **280**, 95–102.
15. Jing, G., Wang, L., Yu, H., Amer, W. A. & Zhang, L. [2013]: Recent progress on study of hybrid hydrogels for water treatment. *Colloids Surfaces A Physicochem. Eng. Asp.* **416**, 86–94.
16. Soleimani, K., Tehrani, A. D. D. & Adeli, M. [2018]:Bioconjugated graphene oxide hydrogel as an effective adsorbent for cationic dyes removal. *Ecotoxicol. Environ. Saf.* **147**, 34–42.
17. Hu, X. S., Liang, R. & Sun, G. [2018]:Super-adsorbent hydrogel for removal of methylene blue dye from aqueous solution. *J. Mater. Chem. A* **6**, 17612–17624.
18. Nesrinne, S. & Djamel, A. [2017]:Synthesis, characterization and rheological behavior of pH sensitive poly(acrylamide-co-acrylic acid) hydrogels. *Arab. J. Chem.* **10**, 539–547.
19. Naficy, S., Razal, J. M., Spinks, G. M., Wallace, G. G. & Whitten. [2012]: P. G. Electrically conductive, tough hydrogels with pH sensitivity. *Chem. Mater.* **24**, 3425–3433.
20. Zheng, Y., Cheng, B., Fan, J., Yu, J. & Ho, W. [2021]:Review on nickel-based adsorption materials for Congo red. *J. Hazard. Mater.* **403**, 123559.
21. Yilmaz, E., Guzel Kaya, G. & Deveci, H. [2019]:Removal of methylene blue dye from aqueous solution by semi-interpenetrating polymer network hybrid hydrogel: Optimization through Taguchi method. *J. Polym. Sci. Part A Polym. Chem.* **57**, 1070–1078.
22. Mudassir, M. A. *et al.* [2019]:Magnetic Hierarchically Macroporous Emulsion-Templated Poly(acrylic acid)-Iron Oxide Nanocomposite Beads for Water Remediation. *Langmuir* **35**, 8996–9003.
23. Pang, J. *et al.* [2019]:Transition metal carbide catalysts for biomass conversion: A review. *Appl. Catal. B Environ.* **254**, 510–522.
24. Rehman, T. U., Shah, L. A., Khan, M., Irfan, M. & Khattak, N. S. [2019]: Zwitterionic superabsorbent polymer hydrogels for efficient and selective removal of organic dyes. *RSC Adv.* **9**, 18565–18577.
25. Agnihotri, S. & Singhal, R. [2019]:Effect of Sodium Alginate Content in Acrylic Acid/Sodium Humate/Sodium Alginate

Superabsorbent Hydrogel on Removal Capacity of MB and CV Dye by Adsorption. *J. Polym. Environ.* **27**, 372–385.

26. Soldatkina, L. & Zavrichko, M.[2019]: Equilibrium, kinetic, and thermodynamic studies of anionic dyes adsorption on corn stalks modified by cetylpyridinium bromide. *Colloids and Interfaces* **3**.
27. Varaprasad, K., Reddy, N. N., Ravindra, S., Vimala, K. & Raju, K. M. [2011]: Synthesis and characterizations of macroporous poly(acrylamide-2- acrylamido-2-methyl-1-propanesulfonic acid) hydrogels for in vitro drug release of ranitidine hydrochloride. *Int. J. Polym. Mater. Polym. Biomater.* **60**, 490–503.
28. Chowdhury, N. *et al.* [2021]:Role of Ionic Moieties in Hydrogel Networks to Remove Heavy Metal Ions from Water. *ACS Omega* **6**, 836–844.
29. Khandaker, S., Toyohara, Y., Saha, G. C., Awual, M. R. & Kuba, T. [2020]:Development of synthetic zeolites from bio-slag for cesium adsorption: Kinetic, isotherm and thermodynamic studies. *J. Water Process Eng.* **33**, 101055.
30. Farghali, A. A., Bahgat, M., Enaiet Allah, A. & Khedr, M. H. [2013]: Adsorption of Pb(II) ions from aqueous solutions using copper oxide nanostructures. *Beni-Suef Univ. J. Basic Appl. Sci.* **2**, 61–71.
31. Feng, Y. Y., Jiang, C. F., Liu, D. J. & Chu, W. [2014]:Microstructure and its influence on CH4 adsorption behavior of deep coal. *Chinese Phys. B* **23**, 1–7.
32. Zhang, H., Feng, J., Li, L., Jiang, Y. & Feng, J. [2019]: Controlling the microstructure of resorcinol-furfural aerogels and derived carbon aerogels: Via the salt templating approach. *RSC Adv.* **9**, 5967–5977.
33. Atta, A. M. *et al.* [2019]:Hybrid ionic silver and magnetite microgels nanocomposites for efficient removal of methylene blue. *Molecules* **24**.
34. Stawskiid, D. & Nowak, A. [2019]:Thermal properties of poly(N,N-dimethylaminoethylmethacrylate),doi:10.1371/journal.pone.0217441.
35. Alwattar, A. A. *et al.*[2020] :Heavy metal sensors and sequestrating agents based on polyaromatic copolymers and hydrogels, doi:10.1002/pi.6086.
36. Ni, H. *et al.* [2017]:Preparation of a poly(DMAEMA-co-HEMA) self-supporting microfiltration membrane with high anionic permselectivity by electrospinning. *E-Polymers* **17**, 149–157.
37. Kress, P., Nägele, H. J., Oechsner, H. & Ruile, S. [2018]:Effect of agitation time on nutrient distribution in full-scale CSTR biogas digesters. *Bioresour. Technol.* **247**, 1–6.

38. Chatterjee, S., Chatterjee, S., Chatterjee, B. P. & Guha, A. K. [2007]: Adsorptive removal of congo red, a carcinogenic textile dye by chitosan hydrobeads: Binding mechanism, equilibrium and kinetics. *Colloids Surfaces A Physicochem. Eng. Asp.* **299**, 146–152.
39. Chatterjee, S., Lee, D. S., Lee, M. W. & Woo, S. H. [2009]: Enhanced adsorption of congo red from aqueous solutions by chitosan hydrogel beads impregnated with cetyl trimethyl ammonium bromide. *Bioresour. Technol.* **100**, 2803–2809.
40. Jiang, C., Fu, B., Cai, H. & Cai, T. [2016]: Efficient adsorptive removal of Congo red from aqueous solution by synthesized zeolitic imidazolate framework-8. *Chem. Speciat. Bioavailab.* **28**, 199–208.
41. Azizian, S., Eris, S. & Wilson, L. D. [2018]: Re-evaluation of the century-old Langmuir isotherm for modeling adsorption phenomena in solution. *Chem. Phys.* **513**, 99–104.
42. Karagöz, S., Tay, T., Ucar, S. & Erdem, M. [2008]: Activated carbons from waste biomass by sulfuric acid activation and their use on methylene blue adsorption. *Bioresour. Technol.* **99**, 6214–6222.
43. Balarak, D., Mostafapour, F., Azarpira, H. & Joghataei, A. [2017]: Langmuir, Freundlich, Temkin and Dubinin–radushkevich Isotherms Studies of Equilibrium Sorption of Ampicilin unto Montmorillonite Nanoparticles. *J. Pharm. Res. Int.* **20**, 1–9.
44. Ho, Y. S. & McKay, G. [1999].Pseudo-second order model for sorption processes. *Process Biochem.* **34**, 451–465.
45. Nakhjiri, M. T., Bagheri Marandi, G. & Kurdtabar, M. [2019]:Adsorption of Methylene Blue, Brilliant Green and Rhodamine B from Aqueous Solution Using Collagen-g-p(AA-co-NVP)/Fe 3 O 4 @SiO 2 Nanocomposite Hydrogel. *J. Polym. Environ.* **27**, 581–599.
46. Zhou, J., Hao, B., Wang, L., Ma, J. & Cheng, W.[2017]:Preparation and characterization of nano-TiO2/chitosan/poly(N-isopropylacrylamide) composite hydrogel and its application for removal of ionic dyes. *Sep. Purif. Technol.* **176**, 193–199.
47. Abdulwahid, A. A. *et al* [2021*]:*An efficient reusable perylene hydrogel for removing some toxic dyes from contaminated water. *Polym. Int.* **70**, 1234–1245.
48. Erdem, M., Yüksel, E., Tay, T., Çimen, Y. & Türk, H. [2009]:Synthesis of novel methacrylate based adsorbents and their sorptive properties towards p-nitrophenol from aqueous solutions. *J. Colloid Interface Sci.* **333**, 40–48.
49. Gupta, V. K., Mittal, A. & Gajbe, V.[2005]:Adsorption and desorption studies of a water soluble dye, Quinoline Yellow, using

waste materials. *J. Colloid Interface Sci.* **284**, 89–98.

50. Zhao, B., Xiao, W., Shang, Y., Zhu, H. & Han,R.[2017]:Adsorption of light green anionic dye using cationic surfactant-modified peanut husk in batch mode. *Arab. J. Chem.* **10**, S3595–S3602.
51. Omini, J. J. *et al.* [2021]:Removal of Carcinogenic Dyes Congo red (CR) and Bismarck brown Y (BBY) by Adsorption onto Reusable Hydrogels Derived from Acrylamide You may also like Synthesis of polyacetone acrylamide and detection of amine benzene Wenting Song and Nanjie Mei-Sodium Chloride Inhibits Acrylamide Formation During Deep Fat Frying Of Plantain Removal of Carcinogenic Dyes Congo red (CR) and Bismarck brown Y (BBY) by Adsorption onto Reusable Hydrogels Derived from Acrylamide. *J. Phys* 12011 doi:10.1088/1742-6596/2063/1/012011.
52. Elgarahy, A. M., Elwakeel, K. Z., Mohammad, S. H. & Elshoubaky, G. A.[2021]: A critical review of biosorption of dyes, heavy metals and metalloids from wastewater as an efficient and green process. *Clean. Eng. Technol.* **4**, 100209.